Journal of Advanced Scientific Research
Available online through https://sciensage.info
ISSN
0976-9595
Research Article

SPECTROSCOPIC, MOLECULAR STRUCTURE, FMO AND THERMODYNAMIC PROPERTIES OF 11-CHLORO-12(METHYLSULFANYL) QUINOXALINE MOLECULE USING DFT

Sushma G. N., Suma M., Wajeeha Sultana, Y. F. Nadaf *

Department of Physics and Materials Research Center, Maharani Science College for Women, Maharani Cluster University, Bengaluru, India

**Corresponding author: dryfnadaf@gmail.com*

Received: 25-01-2022; Revised: 29-04-2022; Accepted: 12-05-2022; Published: 31-05-2022

 https://doi.org/10.55218/JASR.202213410

ABSTRACT

In this article theoretical DFT work on quinoxaline derivative is reported. Quantum mechanical calculations of different energies components of 11-Chloro-12(Methylsulfanyl) Quinoxaline [11Cl12MsQ] in ground state were carried out by DFT method, in isolated state and in different solvents to study the effects of solvents on various energy components. The influence of these solvents on optimized geometry, Mulliken charge distribution in ground and excited state were studied. With the help of computed highest occupied molecular orbital (HOMO) - lowest unoccupied molecular orbital (LUMO) gap of 11Cl12MsQ in different medium we can compute solvation energy, ionization potential, electron affinity, chemical hardness, electron chemical potential, electronegativity and global electrophilicity. UV-Vis spectrum and emission energy were analysed using TDDFT method. The density distribution analysis by total electron density (TED), potential distribution over molecule by electrostatic potential (ESP) positions of 11Cl12MsQ were analysed from molecular electrostatic potential (MEP) and frontier molecular orbitals (FMO) analysis. Thus, our objective is to determine their electronic, thermodynamic and spectroscopic parameters on the basis of the DFT quantum chemical analysis and also studying the effect of solvent and solute-solvent interactions. The structural, electronic and optical properties for quinoxaline derivative helps in better understanding of molecule in different medium which helps us to study biological properties of the molecule. This compound could be useful for designing of optoelectronic devices.

Keywords: Quinoxaline derivative, Mulliken, UV-Vis, Emission energy, Thermodynamic, FMO.

1. INTRODUCTION

Quinoxaline and its derivatives have considerable attention from many years due to their versatile uses in the field of biomedicine and pharmacology. Quinoxaline derivatives shows activities like antibacterial, antifungi, leishmania, tuberculosis, malaria, cancer, depression, neurological and metabolic disease treatment [1-3], quinoxaline derivatives may use in electroluminescent materials [4-6]. Many quinoxaline derivatives are artificial and echinomycin and triostin-A are natural quinoxaline derivatives. Therefore, the condensation of o-phenylenediamine with α-dicarbonyl compounds outcomes in quinoxaline formation [7-8].

According to the literature survey, no theoretical studies have been carried out for 11-Chloro-12(Methylsulfanyl) Quinoxaline [11Cl12MsQ]. We are doing a detailed theoretical study of 11Cl12MsQ using Density Functional Theory (DFT) and Time-Dependent Density Functional Theory (TD-DFT) which were treated according to Becke's three Lee–Yang– Parr (B3LYP) gradient correlation potential and all evaluation were finished with the aid of basis set 6-311G (d, p) [9-11]. DFT and TDDFT are used to simulate the optical parameters of each organic and inorganic molecules, DFT is implemented for studying the ground state (GS) parameters of molecule and TD-DFT used for modeling the energies, systems and properties of electronically excited states (ES) [12], DFT presents the theoretical prediction of molecular drug designing and allows us to understanding the chemical methods in organic structures [13].

Hence, an attempt has been made to do the systematic investigation of geometrical properties, thermodynamic properties, structural properties, frontier molecular

orbital analysis, total electron density (TED), electrostatic potential (ESP), molecular electrostatic potential (MEP) of 11Cl12MsQ with the help of quantum chemical calculations [14, 15]. Furthermore, optical (absorption and emission) was performed with TDDFT in order to explain differences due to liquid and gas phase. Hence, in this present work, we observe that, the obtained band gap is in good agreement with semiconducting material which can be used in designing of optoelectronic devices and these quantum chemical calculations of molecule in gas and liquid phase shows the positive actions towards the biological activities.

2. COMPUTATIONAL METHODS

The calculations on 11Cl12MsQ have been carried out by building its structure using Gauss view 5.0 and Gaussian 09 W software package is used to do all theoretical studies included in the article. Initially the geometry became optimized by means of DFT with B3LYP functional and 6-311G (d, p) basis set, the atomic charge distribution in the ground state and TDDFT in the excited state [16], thermodynamic properties, structural properties and optical properties were studied the use of DFT method B3LYP/6-311G (d, p) and frontier molecular orbital analysis of titled molecule in vacuum and liquid phase was studied.

The thermodynamic properties like SCF energy, enthalpy, entropy, dipole moment, zero-point vibrational energy, heat capacity and rotational constants are calculated. UV-Vis and emission spectroscopic studies have done for 11Cl12MsQ molecule in different medium and recorded the energy maximum with oscillatory strength using TDDFT method with B3LYP/6-311G (d, p) level of study. The energy values in different molecular orbitals of HOMO and LUMO is noted in different medium and the energy separation between these molecular orbital is prolonged to simulate various molecular factors like ionization ability, electron chemical capacity, electronegativity, electron affinity, chemical hardness, and international electrophilic index and so on, TED surface mapping, ESP, MEP and contour mapping of the titled molecule in vacuum and solvent medium is determined using DFT method. Thus, in this present work, our primary aim is to perform a complete theoretical study on the 11Cl12MsQ molecule [17].

3. RESULTS AND DISCUSSION

3.1. Structure and geometric properties

The designed structure of 11Cl12MsQ from the gauss view is geometrically optimized by using Gaussian 09 with keyword opt, B3LYP functional and 6-311G (d, p) basis set [18]. Initial geometry generated from standard parameters which are then reduced to a minimum by the Gaussian program which computes the energies to discover the molecular geometry similar to the minimum energy. The optimized molecular geometries of 11Cl12MsQ are illustrated in Fig.1 [19].

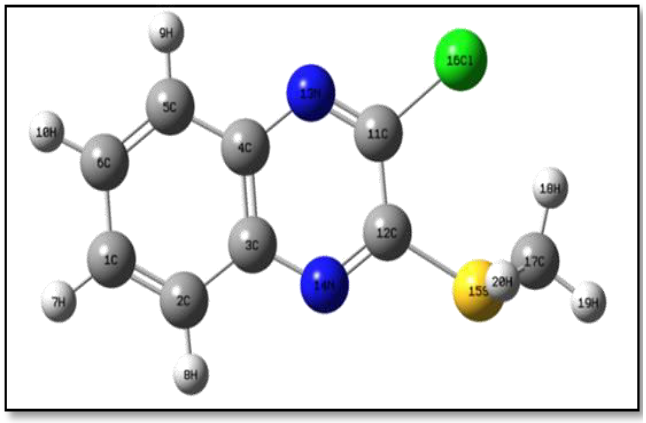

Fig. 1: Optimized molecular Structure of 11-chloro-12-(methylsulfanyl) quinoxaline

The ground and excited geometries of the molecule was studied by using DFT/B3LYP/6-311G (d, p) and TDDFT/B3LYP/6-311G (d, p) level respectively. The geometrical parameters have been given in Table 1, bond length increased from ground to excited state in, 18H-17C with 0.000001 Å at the same time as shortened in 11C–7H, 13N-11C and 20H-17C with zero.000001 Å. The bond angles lengthened from ground to excited state in 9H-5C-4C and 11C-7H-3C even as shortened in 5C-4C-3C, 7H-1C-2C and 12C-11C-4C. The trade toward lengthening has been located to be 0.0001 and 0.00003 respectively, while shortening has been located for 5C-4C-3C, 7H-1C-2C is 0.0001° and 12C-11C-4C is 0.00003°. Significant torsion for the excited state has been received for the 4C-3C-2C-1C, 5C-4C-3C-2C, 6C-5C-4C-3C, 13N-11C-4C-3C, 16Cl-11C-4C-3C and 19H-17C-15S-12C dihedral angles which can be more twisted than the ground state, while 12C-11C-4C-3C and 14N-12C-11C-4C dihedral angles are extra twisted on the ground state and torsion decreased on the excited state [14, 20].

3.2. Mulliken atomic charge distribution

Mulliken atomic charge distributions on each atomic site of 11Cl12MsQ were investigated using DFT/B3LYP/6-311G (d, p) in vacuum medium, toluene and methanol solvents. Mulliken charge distribution of each atom of 11Cl12MsQ is shown in Table 2 and charge distribution in different medium is represented graphically as shown in Fig. 2. The solvent influences of on the atomic charges are observed from the analysis. The atomic charges increase with increasing solvent polarity from toluene to methanol, the values of atomic charges in methanol are higher variation than in vacuum and toluene. For 11Cl12MsQ in vacuum with atom number (C1, C2, C5, C6, C12, C17) carbon atoms, (N13, N14) nitrogen atoms, (Cl16) Chlorine atom which are associated with a negative charge which indicates that these are donor atoms, whereas (C3, C4, C11) carbon atoms, (S15) sulphur atom and all hydrogen atoms acts as an acceptor. In toluene medium, there is a slight increase in atomic charge of hydrogen atoms, increase in atomic charge of most carbon atoms, there is increase in charge of (N13, N14) nitrogen atoms from vacuum to toluene medium. In methanol medium, the atomic charge distribution of all carbon atoms, hydrogen atoms and nitrogen atoms are higher than vacuum and toluene medium, there is slight increase in (Cl16) chlorine atom from vacuum to toluene and toluene to methanol. Similar trend is found in C466 molecule [21].

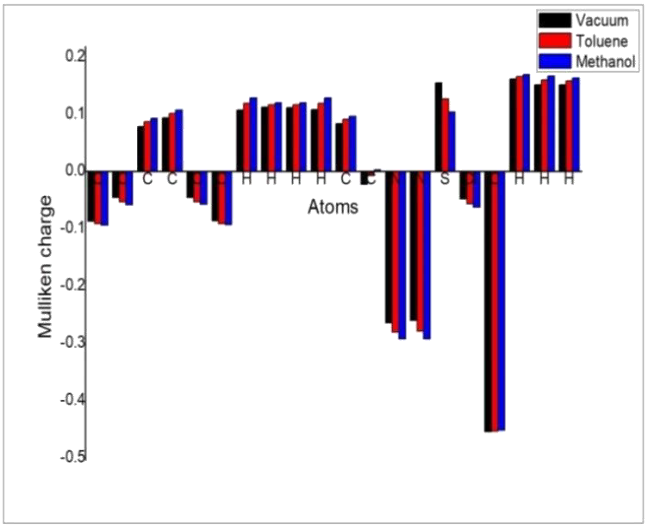

Fig. 2: Mulliken atomic charge distribution of 11Cl12MsQ in vacuum, toluene and methanol medium using DFT method

Table 1: Bond length (Å), Bond angle (°) and dihedral angle of 11Cl12MsQ using DFT/B3LYP/6-311G (d, p) and TDDFT/ B3LYP/6-311G (d, p)

Atoms	Bond length (Å)		Atoms	Bond Angle (°)		Atoms	Dihedral Angle	
	Ground State	Excited state		Ground State	Excited state		Ground State	Excited state
2C-1C	1.375018	1.375018	3C-2C-1C	119.6465	119.6465	4C-3C-2C-1C	-0.36236	-0.3624
3C-2C	1.414564	1.414564	4C-3C-2C	119.5053	119.5053	5C-4C-3C-2C	0.414666	0.414738
4C-3C	1.422684	1.422684	5C-4C-3C	119.8435	119.8434	6C-5C-4C-3C	-0.19339	-0.19344
5C-4C	1.41263	1.41263	6C-5C-4C	119.4852	119.4852	7H-1C-2C-3C	-179.858	-179.858
6C-5C	1.375646	1.375646	7H-1C-2C	119.9318	119.9317	8H-2C-1C-6C	179.7489	179.7489
7H-1C	1.083819	1.083819	8H-2C-1C	122.2779	122.2779	9H-5C-4C-3C	-179.939	-179.939
8H-2C	1.082952	1.082952	9H-5C-4C	118.2806	118.2807	10H-6C-5C-4C	-179.96	-179.96
9H-5C	1.082937	1.082937	10H-6C-5C	119.8596	119.8596	11C-7H-3C-2C	-179.078	-179.078
10H-6C	1.083863	1.083863	11C-7H-3C	89.7416	89.74163	12C-11C-4C-3C	-2.10216	-2.10214
11C-7H	2.275158	2.275157	12C-11C-4C	91.35113	91.35111	13N-11C-4C-3C	179.2895	179.2896
12C-11C	1.444444	1.444444	13N-11C-4C	31.9481	31.9481	14N-12C-11C-4C	1.968987	1.968981
13N-11C	1.291941	1.29194	14N-12C-11C	119.1249	119.1249	15S-12C-11C-4C	176.5878	176.5878
14N-12C	1.309974	1.309974	15S-12C-11C	124.695	124.695	16Cl-11C-4C-3C	173.7413	173.7414
15S-12C	1.791726	1.791726	16Cl-11C-4C	148.0432	148.0432	17C-15S-12C-11C	63.36807	63.36807
16Cl-11C	1.761913	1.761913	17C-15S-12C	103.0164	103.0164	18H-17C-15S-12C	-68.1758	-68.1758
17C-15S	1.833838	1.833838	18H-17C-15S	112.2187	112.2187	19H-17C-15S-12C	173.2504	173.2505
18H-17C	1.087487	1.087488	19H-17C-15S	104.8156	104.8156	20H-17C-15S-12C	56.09378	56.09378
19H-17C	1.090571	1.090571	20H-17C-15S	110.3973	110.3973	-	-	-
20H-17C	1.089308	1.089307	-	-	-	-	-	-

Table 2: Mulliken atomic charges by DFT/ B3LYP/6-311G (d,p) in vacuum and solvent medium

No.	Atoms	Mulliken Charge		
		Vacuum	Toluene	Methanol
1	C	-0.086727	-0.091553	-0.09338
2	C	-0.04563	-0.05295	-0.05844
3	C	0.078348	0.087183	0.093274
4	C	0.093871	0.101743	0.1071
5	C	-0.04569	-0.05256	-0.05745
6	C	-0.0862	-0.09092	-0.09266
7	H	0.107565	0.119143	0.128215
8	H	0.111986	0.11666	0.119617
9	H	0.111499	0.116769	0.120378
10	H	0.1079	0.119544	0.128701
11	C	0.083463	0.091461	0.096613
12	C	-0.0225	-0.0075	0.002856
13	N	-0.26465	-0.28042	-0.29207
14	N	-0.26041	-0.27854	-0.29237
15	S	0.154866	0.127144	0.104107
16	Cl	-0.04802	-0.05623	-0.0626
17	C	-0.4546	-0.45324	-0.45152
18	H	0.161986	0.165784	0.169068
19	H	0.151551	0.160239	0.166828
20	H	0.151387	0.158248	0.163746

3.3. Thermodynamic parameters

Thermodynamic parameters are very useful for knowing the chemical processes. The DFT is a very useful tool for studying statistical thermodynamic properties of the molecules, translational energy, rotational energy, vibrational energy, total energy, nuclear repulsion energy, zero-point vibrational energy and the statistical thermodynamic parameters, such as, entropy (S), rotational constants and temperatures, molecular capacity of constant volume, dipole moment were found from the theoretical harmonic frequencies calculated by DFT/B3LYP/6-311G (d, p) level of theory for the 11Cl12MsQ molecule at temperature of 298.15 K and 1 atm pressure and given in Table 3. The thermodynamic parameters calculated here give available information for further studies on the 11Cl12MsQ molecule [22].

3.4. Absorption and emission spectroscopic study

TDDFT has been used to discover the excited states of 11Cl12MsQ in vacuum, toluene and methanol medium as shown in Table 4. Results related to the vertical excitation energies, oscillatory strength (f) and wavelength have been accomplished. The TDDFT has been used to examine the absorption spectra that have been furnished an efficient approach [23, 24], the TDDFT calculation predicts one intense digital transition at 373.79 nm with an oscillator strength f = 0.0546 in vacuum, 369.66 nm with f = 0.0905 in toluene, 363.47 nm with f = 0.0844 in methanol which are shown in Fig. 3.

Table 3: Calculated thermodynamic parameters of 11Cl12MsQ with DFT theory using the B3LYP/6-311G (d, p) basis set

Parameters	DFT/B3LYP/ 6-311G (d, p)
Energy(kcal mol^{-1})	
Translational	0.889
Rotational	0.889
Vibrational	94.170
Total	95.947
Nuclear repulsion energy (Hartree's)	925.7136
Zero-point vibrational energy (kcal mol^{-1})	88.8576
Entropy, S(Cal/Mol-Kelvin)	106.841
Molecular capacity of constant volume (cal mol^{-1} k^{-1})	
Translational	2.981
Rotational	2.981
Vibrational	36.440
Total	42.401
Rotational constants (GHz)	
A	1.28327
B	0.41308
C	0.32442
Rotational temperatures (Kelvin)	
A	0.06159
B	0.01982
C	0.01557
Dipole moment (Debay)	2.428

Table 4: Theoretical Excitation and emission studies of 11Cl12MsQ molecule in vacuum and solvent medium using TDDFT/B3LYP/6-311G (d, p)

	Vacuum	Toluene	Methanol
Excitation energy (nm)	373.79	369.66	363.47
Emission energy (nm)	387.50	382.00	375.30
Oscillator strength	0.0546	0.0905	0.0844

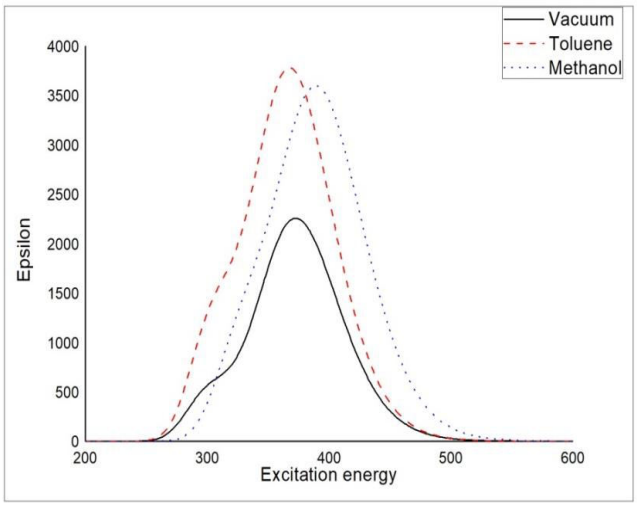

Fig. 3: Absorption spectra of 11Cl12MsQ in vacuum and solvent medium using TDDFT analysis

The estimation of fluorescence access to TD-DFT approach, so that one can optimize the electronically excited-state (EES) geometry, its vertical energies (absorption or emission) with measured longest wavelength of absorption (λ_{max}) is an approximated procedure [25].

The geometry of EES gives to the fluorescence (if the EES is a singlet-state). The emission power of molecule in vacuum medium (387.50 nm) shows higher value as compared to solvent medium.

3.5. Frontier Molecular Orbitals and Quantum chemical calculation

The FMO enables to recognize the electron charge transfer between the donor and acceptor group by the π-conjugate. The HOMO (electron-donating) directly associated with the ionization potential, even as the LUMO (electron-accepting) associated with the electron affinity of the compound. Plot of FMO helps us to have higher information of the nature of the chemical structure and chemical reaction of the molecule [9, 26]. HOMO, HOMO-1, HOMO-2 are the orbitals that present π-bonding symmetry and LUMO, LUMO+1, LUMO+2 (Table 5) are molecular orbitals that shows π* antibonding symmetry. Fig. 4 indicates a 3D representation of frontier molecular orbital in different medium using DFT method with B3LYP functional and 6-311G (d, p) basis set in which greenish area indicates the positive region and reddish area shows the negative region of the molecular orbital.

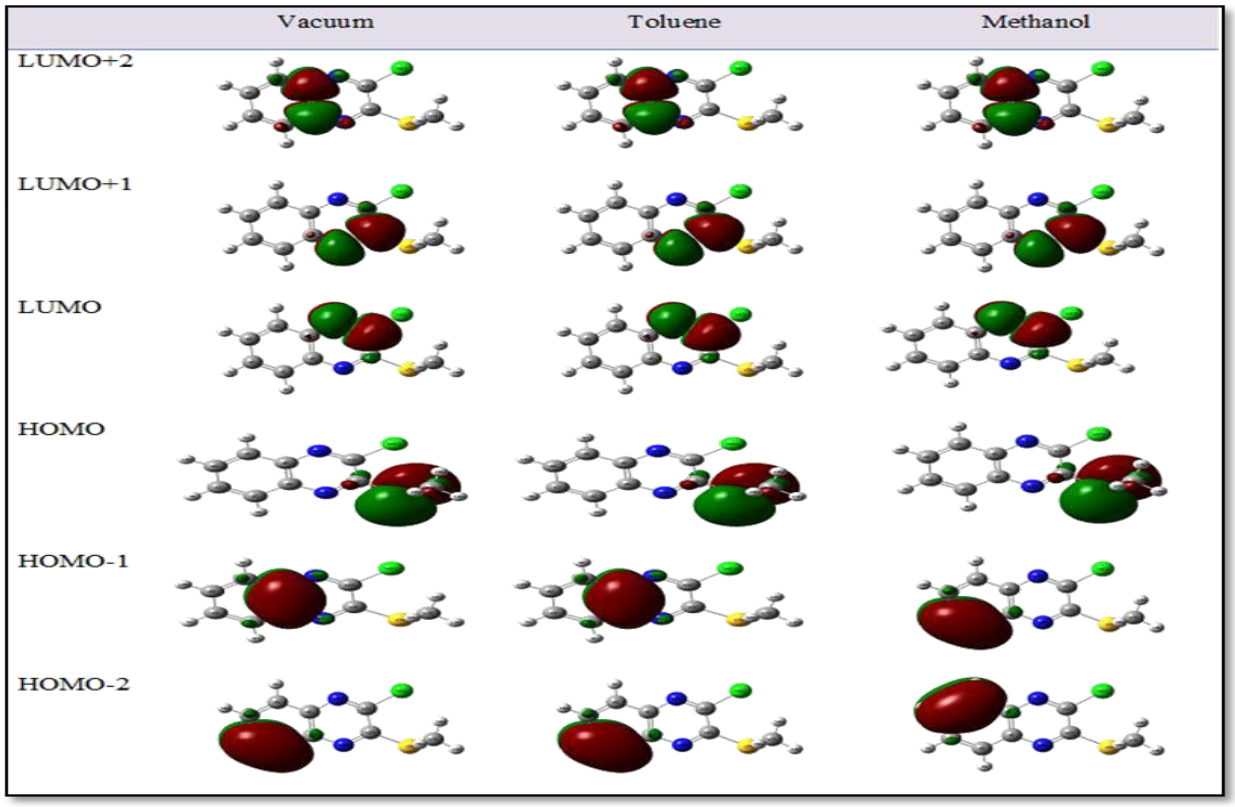

Fig. 4: 3D representation of frontier molecular orbital of 11Cl12MsQ in vacuum and solvent (toluene, methanol) medium using DFT method

Table 5: HOMO and LUMO energy states values of 11Cl12MsQ in vacuum, toluene and methanol medium

Molecular orbital	Energy in eV		
	Vacuum	Toluene	Methanol
LUMO+2	0.1083	0.0982	0.0827
LUMO+1	-0.5989	-0.6514	-0.5442
LUMO	-0.6177	-0.6779	-0.7372
HOMO	-6.8335	-6.9568	-7.0675
HOMO-1	-7.4264	-7.4291	-7.4256
HOMO-2	-7.4936	-7.4571	-7.4283

The energy gap (E_g) has been analysed using the equation (1) given below, which gives energy gap (E_g) between HOMO to LUMO. The E_g in methanol medium shows the largest energy gap of 6.3303 eV, energy gap of HOMO-1 to LUMO+1 is 6.9241 eV and the E_g between HOMO+2 to LUMO-2 is 7.511 eV, which shows that the energy band gap value increases with solvent polarity [27]. By DFT theory of quantum chemical parameters, negative of HOMO energy is taken as ionization potential (I) and negative of LUMO energy as electron affinity (E) can be analysed. I and E are important features of organic molecules and ions, which makes it possible to get the molecular reactivity and interpret the results of electronic spectra [28]. The values of E_g, I and E helps us to analyse the various parameters like chemical hardness (η), chemical potential (μ), chemical softness (s), global electrophilicity (ω) of the probe molecule in vacuum and solvent medium were reported in Table 6 [29].

The energy band gap 'E_g' (=E_{HOMO} ~ E_{LUMO}) can be obtained from HOMO and LUMO, the ability of atoms to attract the shared electrons of a covalent bond gives electronegativity 'χ' (= (I+E)/2), chemical hardness 'η' (= (I-E)/2) is half of the energy band gap, the chemical potential 'μ' is obtained by the negative value of electronegativity (-χ), and chemical softness 's' (= 1/2η), Hence global electrophilicity 'ω' ($\omega=\mu^2/2\eta$) can be analysed [29].

Table 6: Physicochemical properties of 11Cl12MsQ with vacuum and solvents

Solvents	Energy band gap (E_g)	Ionization potential (I)	Electron affinity (A)	Electro negativity (χ)	Chemical hardness (η)	Chemical potential (μ)	Chemical Softness (s)	Global Electrophilicity (ω)
Vacuum	6.2158	6.8335	0.6177	3.7256	3.1079	-3.7256	1.55395	21.56897418
Toluene	6.2789	6.9568	0.6779	3.81735	3.13945	-3.81735	1.569725	22.87428546
Methanol	6.3303	7.0675	0.7372	3.90235	3.16515	-3.90235	1.582575	24.09998309

3.6. ESP, TED and MEP studies

ESP, TED and MEP maps are obtained using DFT theory with B3LYP/6-311G (d, p) model, the 3D plots of these are presented in Fig. 5.

3.6.1. Electrostatic Potential (ESP)

The ESP provides an accurate and beter understanding of intermolecular association molecular properties of the molecule and also it provides knowledge about location of electrophilic and nucliophilic siter. By the ESP study, the energy of molecule ranges in vacuum medium is between -0.2788 eV to 0.2788 eV, in toluene medium -0.2838eV to 0.2838 eV and in methanol from -0.3006 eV to 0.3006 eV are found. The surface map energy in the site of nitrogen atoms. We absorve red color and surrounded by yellow color in Fig.5(a). In the site of N13, the energy values in vacuum, toluene and methanol are -0.268eV, -0.219 eV, -0.2329 eV (red) and -0.1529 eV, -0.140 eV, -0.108 eV (yellow). The energy values in the site of N14 are -0.274 eV, -0.2138 eV, -0.2514 eV (red) and -0.09558 eV, -0.1224 eV, -0.152 eV (yellow) respectively.

3.6.2. Total electron density (TED)

The TED offers essential statistics for expertise the shape, charge, size, delocalization of molecule and location of chemical reactivity of the molecule, TED plots are shown in Fig. 5(b) which shown the uniform distribution [30] for the 11Cl12MsQ molecule in all three medium (vacuum, toluene and methanol).

3.6.3. Molecular electrostatic potential (MEP)

The MEP studies help to know the molecular parameters, charge density and polarity of the compound. Red colour represents the maximum negative potential region, the blue colour represents the maximum positive potential region, green represents the zero potential areas [31]. The 3D MEP mapping of

11Cl12MsQ in vacuum and solvent medium is presented in Fig.5(c). The MEP in different medium shows almost same mapping surfaces with similar type of colour code. The site of nitrogen atoms N13 and N14 are nucliophilic attack regions because of its maximum negative potential. Mesmeric effect of nitro group shows within the area with large electronic charge indicates reddish shade. The 16Cl position is more potential than the nitro groups which are surrounded by yellow colour. However, the hydrogens 7H, 8H, 9H, 10H, 18H, 19H, and 20H represents large positive potential surface and results to an electrophilic attack region with a blue shade surrounding. Electrons within the benzene ring are proven the greenish shade of the molecule. The contour mapping of 11Cl12MsQ molecule in vacuum, toluene and methanol medium were shown in Fig. 5(d).

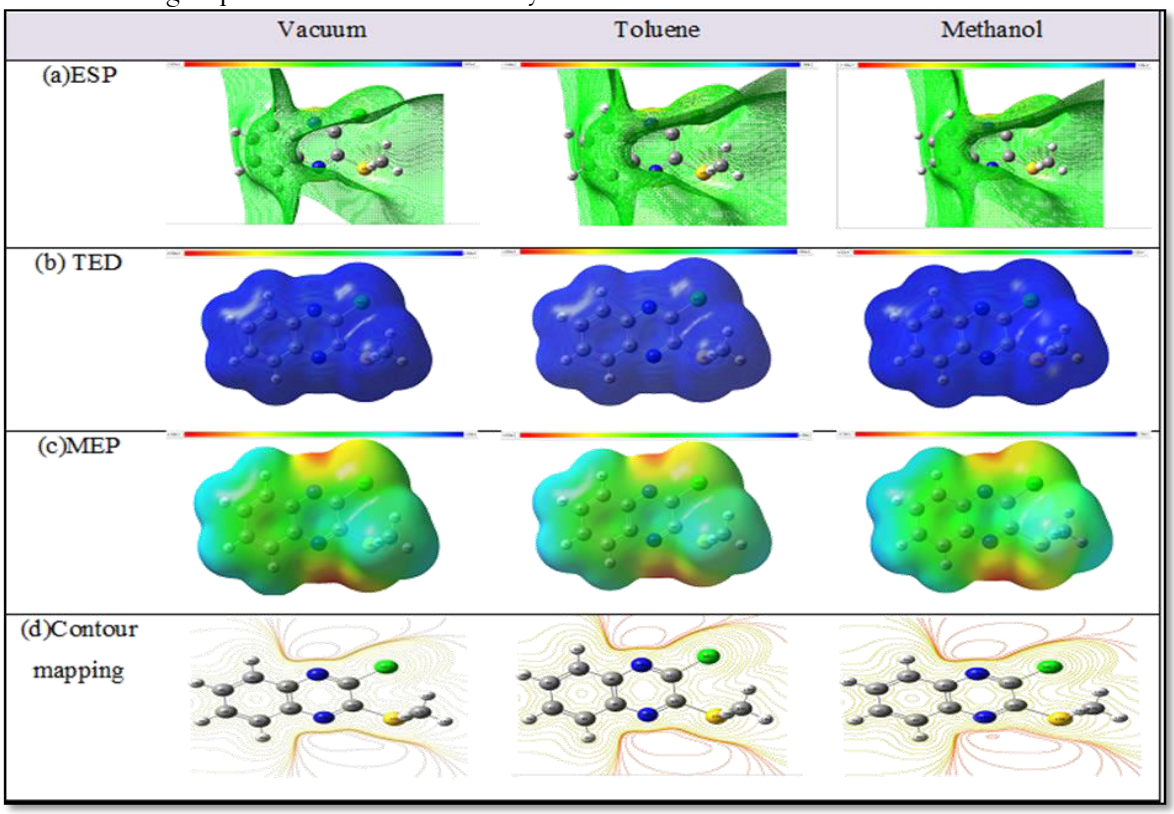

Fig. 5: (a) ESP mapping, (b) TED, (c) MEP surface and (d) contour mapping of11Cl12MsQ in vacuum, cyclohexane and octanol medium

4. CONCLUSION

In this paper, we have implemented a computational approach, which combines DFT and TDDFT strategies to observe the 11Cl12MsQ molecule. The geometry allowes structural properties, when you consider that a few precise distances and angles can impact the orbital overlap and, therefore, the charge transfer absorption. The UV-Visible absorption properties were acquired primarily based on TD-DFT calculations, we discussed the emission spectrum which is likewise called as vertical excitation this is carried out by considering electronic excited energy state as reference and apply the TD-DFT again. The FMO energy gap useful for representing the high chemical reactivity and stability of the compound. A molecule with a less E_g is commonly related to an excessive chemical reactivity, low kinetic stability and is also known as soft molecule. We can conclude that, by detailed theoretical study of 11Cl12MsQ molecule helps in better understanding of molecule in different medium which helps us to study biological properties of the molecule.

5. ACKNOWLEDGEMENT

Authors are thankful to DFT-FIST and UGC-CPE of Maharani Science College for Women, Bengaluru.

Conflict of interest

The authors declared no potential conflicts of interest w.r.t. the research, authorship/publication of this article.

Source of funding
Nil

6. REFERENCES

1. Desmond Brown J, Edward Taylor C, Jonathan Ellman A. The Chemistry of Heterocyclic Compounds: Wiley, New York; 2004.
2. Aparicio D, Attanasi OA, Filippone P, Ignacio R, Lillini S, Mantellini F, Palacios F, de Los Santos JM. *J Org Chem*, 2006; **71(16):**5897-5905.
3. Pradeep, K, Kotra V, Priyadarshini R, Pratap V. *Int J Pharm and Pharmace Sci,* 2014; **7:** 243-246.
4. Sharma, G, Raisinghani PM, Abraham I, Pardasani RT, Mukherjee T. *Indian J Chem*, 2009; **48**.
5. Justin Thomas KR, Velusamy M, Lin JT, Chuen CH, Tao YT. *Chem Materials*, 2005 Apr 5; **17(7):**1860-1866.
6. Chang DW, Ko SJ, Kim JY, Dai L, Baek JB. *Synthetic Metals*, 2012; **162(14):**1169-1176.
7. Pereira JA, Pessoa AM, Cordeiro MN, Fernandes R, Prudêncio C, Noronha JP, et al. *Eur J Med Chem.,* 2015; **97:**664-672.
8. Aguirre G, Cerecetto H, Di Maio R, González M, Alfaro ME, Jaso A, et al. *Bioorg Med Chem Lett.,* 2004; **14(14):**3835-3839.
9. Sivaprakash S, Prakash S, Mohan S, Jose SP. *Heliyon,* 2019; **5(7):** 02149.
10. Barnes EC, Petersson GA, Montgomery JA, Frisch MJ, Martin JM. *J Chem Theory and Comp.* 2009; **5(10):**2687-2693.
11. Gaussview/Gaussian Guide and Exercise Manual, http://users.df.uba.ar/rboc/em3/GAUSSIAN_TRAIN.pdf
12. Becke AD. *J Chem Phys.,* 1996; **104(3):**1040-1046.
13. Miehlich B, Savin A, Stoll H, Preuss H. *Chem Phys Lett.*, 1989; **157(3):**200-206.
14. Lee C, Yang W, Parr RG. *Physical Rev B.*, 1988; **37(2):**785.
15. El-Daly SA, Asiri AM, Obeid AY, Khan SA, Alamry KA, Hussien MA, Al-Sehemi AG. *Opt and Laser Tech.,* 2013; **45:**605-612.
16. Khajuria Y, Gupta U, Singh S. *Mat Focus*, 2015; **4(5):**385-391.
17. Alande BD, Renuka CG, Sushma GN, Suma M, Basavaraj Sannakki, Nadaf YF. *AIP Conf Proce.,* 2019; **(Vol. 2100, No. 1, p. 020110)** AIP Publishing LLC.
18. Babu NS, Lelisho TA. *Adv. Appl. Sci. Res.*, 2012; **3(6):**3916-3934.
19. Young D. Computational Chemistry: a practical guide for applying techniques to real world problems. John Wiley and Sons; 2004.
20. Liu X, Cole JM, Chow PC, Zhang L, Tan Y, Zhao T. *J Phy Chem C*; **118(24):**13042-13051.
21. Renuka CG, Nadaf YF, Sriprakash G, Rajendra Prasad S. *J Fluor.*, 2018; **28(3):**839-854.
22. Khajuria Y, Sharma S, Gupta U, Singh S. *Mat Focus.*, 2015; **4(5):**338-345.
23. Zhang C, Liang W, Chen H, Chen Y, Wei Z, Wu Y. *J Mol Struct (Thermochem),* 2008; **862(3):**98-104.
24. Matthews D, Infelta P, Grätzel M. *Solar Energy Mat Solar Cells,* 1996; **44(2):**119-155.
25. Renuka CG, Shivashankar K, Boregowda P, Bellad SS, Muregendrappa MV, Nadaf YF. *J Soln Chem.,* 2017; **46(8):**1535-1555.
26. Adamo C, Jacquemin D. *Chem Soc Rev.,* 2013; **42(3):**845-856.
27. Vaz WF, Custodio JM, Rodrigues NM, Santin LG, Oliveira SS, Gargano R, et al. *J Mol Modeling*, 2017; **23(11):**1-3.
28. Siddlingeshwar B, Kirilova EM, Belyakov SV, Divakar DD, Alkheraif AA. *Photochem Photobio Sci.,* 2018; **17(4):**453-64.
29. Sushma GN, Suma M, Pramod AG, Nadaf YF. *AIP Conf Proce.*, 2020 (**Vol. 2220, No. 1, p. 130027)**. AIP Publishing LLC.
30. Pramod AG, Nadaf YF, Renuka CG. *J Mol Struct.*, 2019; **1194:**271-83.
31. Pramod AG, Nadaf YF, Renuka CG. *Spectrochem Acta Part A: Mol and Biomol Spec.,* 2019; **223:**117288.